Y.-M. Sun
W. Liu
R.-H. Zhu
C. Goudet
J. Tytgat
D.-C. Wang

Roles of disulfide bridges in scorpion toxin BmK M1 analyzed by mutagenesis

Authors' affiliations:
Y.-M. Sun, *W. Liu*, *R.-H. Zhu* and *D.-C. Wang*, Center for Molecular Biology, Institute of Biophysics, Chinese Academy of Sciences, Beijing, China.

C. Goudet and *J. Tytgat*, Laboratory of Toxicology, University of Leuven, Leuven, Belgium.

Correspondence to:
Da-Cheng Wang
Center for Molecular Biology
Institute of Biophysics
Chinese Academy of Sciences
15 Datun Road, Chaoyang District
Beijing 100101
China
Tel.: 86-10-6488-8547
Fax: 86-10-6488-8560
E-mail: dcwang@sun5.ibp.ac.cn

Dates:
Received 22 March 2002
Revised 28 May 2002
Accepted 16 July 2002

To cite this article:
Sun, Y.-M., Liu, W., Zhu, R.-H., Goudet, C., Tytgat, J., & Wang, D.-C. Roles of disulfide bridges in scorpion toxin BmK M1 analyzed by mutagenesis.
J. Peptide Res., 2002, **60**, 247–256.

ISSN 1397–002X

Key words: BmK M1; disulfide bridge; mutagenesis analysis; mutant; scorpion toxin

Abstract: The unique fold of scorpion toxins is a natural scaffold for protein engineering, in which multiple disulfide bonds are crucial structural elements. To understand the respective roles of these disulfide bridges, a mutagenesis analysis for the four disulfide bonds, 12–63, 16–36, 22–46 and 26–48, of a representative toxin BmK M1 from the scorpion *Buthus martensii* Karsch was carried out. All cysteines were replaced by serine with double mutations. The recombinant mutants were expressed in the *Saccharomyces cerevisiae* S-78 system. Toxic activities of the expressed mutants were tested on ICR mice *in vivo* and on neuronal Na^+ channels ($rNa_v1.2$) by electrophysiological analysis. Recombinant variants M1 (C22S,C46S) and M1 (C26S,C48S) were not expressed at all; M1 (C16S,C36S) could be expressed at trace levels but was extremely unstable. Variant M1 (C12S,C63S) could be expressed in an amount comparable with that of unmodified rBmK M1, but had no detectable bioactivities. The results indicated that among the four disulfide bonds for long-chain scorpion toxins, loss of either bridge C22–C46 or C26–C48 is fatal for the general folding of the molecule. Bridge C16–C36 mainly contributes to the global stability of the folded scaffold, and bridge C12–C63 plays an essential role in the functional performance of scorpion toxins.

Abbreviations: BmK, *Buthus martensii* Karsch; CD, circular dichroism; PCR, polymerase chain reaction

Scorpion toxins are a complicated small protein family. They demonstrate various species-level specificity, different potency and distinct receptor-binding specificity. Essentially, these toxins act on a diversity of ion channels, including sodium channels (1), potassium channels (2) and chloride channels (3). They have been divided into two

structural classes. The long-chain toxins consist of 60–70 residues cross-linked by four disulfide bridges and act on sodium channels (4), whereas the short-chain toxins are composed of ≈30–40 residues with three or four disulfide bonds and bind to potassium and chloride channels (2,5). To date, eight X-ray crystal structures and nearly 20 NMR solution structures have been deposited into the Protein Data Bank (http://www.rcsb.org/pdb). Detailed comparisons revealed that all these structures adopt a common molecular scaffold comprising a stretch of α-helix and an antiparallel triple-stranded β-sheet (6–10), irrespective of their size, amino acid sequence and function. This general fold is also adopted by some other proteins with divergent function, such as insect defensins (11), plant γ-thionins (12), and sweet-tasting Brazzein (13,14). Therefore, the unique fold of scorpion toxins possesses a high permissiveness for protein engineering as a natural scaffold (15,16).

The common structural elements in all these proteins are multiple disulfide bonds, which cross-link the polypeptide chain to provide most of their stabilizing energy. Therefore, the disulfide bridges are crucial for the scaffold of scorpion toxins. Understanding the role of disulfide bonds in this native scaffold is significant for manipulation of this scaffold, especially for designing minimized proteins expressing new function. Here we report a mutagenesis analysis of the four disulfide bonds in a scorpion toxin, BmK M1.

BmK M1 is a representative neurotoxin of the long-chain toxins from the scorpion *Buthus martensii* Karsch (BmK) that is widely distributed in China and East Asia. It belongs to the long-chain α-like toxins targeting the sodium channel (17,18), and is composed of 64 residues cross-linked by four disulfide bonds. The disulfide bridge motif in BmK M1 follows the pattern (C1–C8, C2–C5, C3–C6, C4–C7) (Fig. 1), which is the common consensus pattern in all long-chain α-toxins (10,19). Thus, taking BmK M1 as a model to understand the respective roles of these disulfide bonds has a general significance. The characterization (20), crystal structure (8) and expression of the encoding gene of this toxin (21) have been carried out in our laboratory. On the basis of these data, double mutations using Ser to replace Cys pairs were used to modify the four disulfide bonds in BmK M1. Mutants were constructed, expressed and characterized, and the significance of these disulfide bonds to structure and function were investigated.

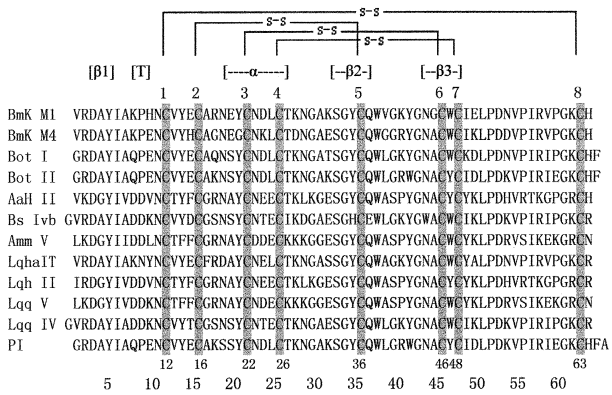

Figure 1. Sequence and consensus pattern of disulfide bonds of BmK M1 in comparison with other long-chain scorpion toxins. The secondary structures are indicated in brackets. The invariant cysteines are highlighted in shadow. Amino acid sequences are from Refs 8,10.

Materials and Methods

Strains, materials and animals

Plasmid pVT 102U/α and *S. cerevisiae* S-78 (Leu^2, Ura^3, Rep^4) yeast strain were used. Restriction endonucleases and T4 DNA ligase were purchased from Roche (Germany). Primers were synthesized by Sangon (Shanghai, China). *Taq* DNA polymerase and Klenow fragment were from MBI (USA). Cation exchanger CM32 cellulose and reversed-phase column Sephasil Peptide C_{18} (12 μm ST 4.6/250) were from Whatman (UK) and Pharmacia Biotech (Sweden), respectively. All other chemicals and reagents were purchased from Merck (Germany) or Sigma (USA).

The mice used for toxicity assays were ICR mice from the Beijing Center for Experimental Animals.

Site-directed mutagenesis of BmK M1

The cDNA of BmK M1 was previously cloned (22) and inserted into pVT 102U/α (21). According to the sequence of recombinant pVT 102U/α-BmK M1, primer 1 (5′-CGTC TAGATAAAAGAAATTCTGTTCGG-3′) including KEX2 linker and *Xba*I restriction site and primer 2 (5′-CGAAGC-TTTTAATGGCATTTTCCTGGTAC-3′) with a *Hin*dIII site were designed. The substitute residues for all cysteines are serine. The sequences of the mutagenic primers used to generate the desired mutations are as follows:

Cys^{12}Ser: 5′-GCCAAGCCCCATAAC**TCT**GTATACGAAT GTGCTAGAAATGAA-3′
Cys^{63}Ser: 5′-CGAAGCTTTTAATG**AGA**ATTTTCCTGGTAC-3′
Cys^{16}Ser: 5′-GTATACGAA**TCT**GCTAGAAAT-3′
Cys^{36}Ser: 5′-TACCCATTG**AGA**ATAGCCACT-3′
Cys^{22}Ser: 5′-AATGAATAT**TCT**AACGATTTA-3′

Cys[46]Ser: 5′-TATGCACCA**AGA**GCCATTTCC-3′
Cys[26]Ser: 5′-AACGATTTA**TCT**ACCAAGAAT-3′
Cys[48]Ser: 5′-ATTATCGGGCAACTCTAT**AGA**CCAGCA GCCATT TCCGTA-3′

Using recombinant pVT 102U/α-BmK M1 (rBmK M1) as template and specific mutagenic primers, mutant (C12S,C63S) was created by one step PCR, whereas variants (C16S,C36S) (C22S,C46S) and (C26S,C48S) were obtained by four-step PCR (Fig. 2). A pair of specific mutagenic primers was applied to amplify a segment, which possessed two desired mutations. After treatment by Klenow fragment, two strands of the segment were applied in the second or third PCR, respectively, with primer 1 and 2 to create two intermediate products, which shared an identical sequence. The three-step PCR above was performed using rBmK M1 as template. After digestion by Klenow fragment, two intermediate products acted as primers to each other and extension of this overlap by DNA polymerase created the full-length mutant which had mutations at the two desired positions. All PCR products were purified by gel excision.

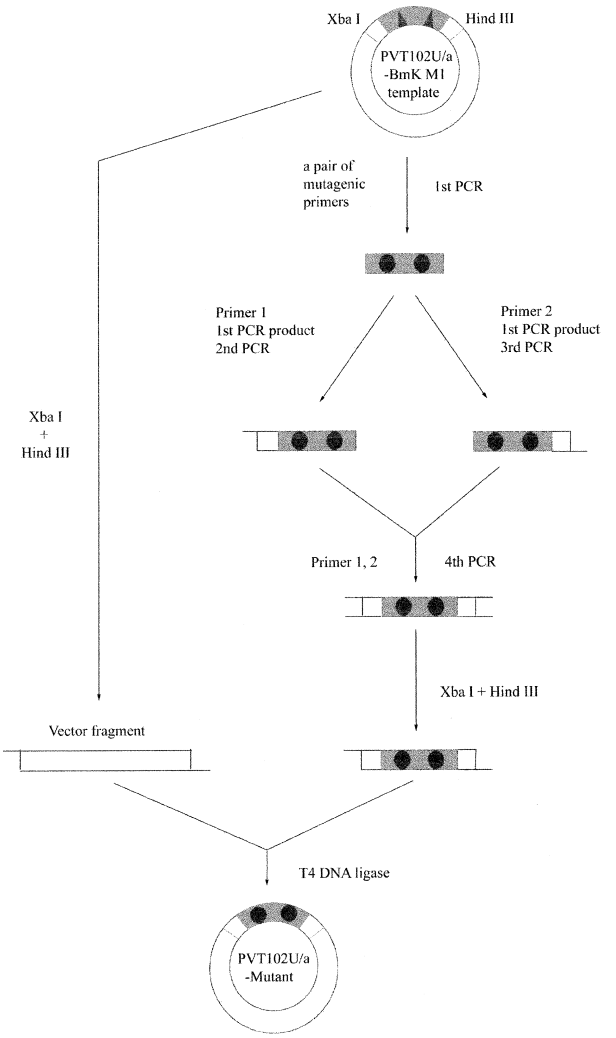

Figure 2. Construction of recombinant plasmid pVT 102U/α-mutants. Four-step PCR for variants (C16S,C36S) (C22S,C46S) and (C26S,C48S) is shown. The designed mutation sites and mutated sites are indicated by filled triangles and circles, respectively. In the first PCR, a pair of specific mutagenic primers is applied to amplify a segment. In the second or third PCR, two separate strands are applied to create two intermediate products, which then create full-length mutants in the fourth PCR. Finally the gene is fused with pVT 102U/α. Variant (C12S,C63S) is created by using a pair of specific mutagenic primers in one step PCR.

Expression and purification of mutants

The mutated cDNA gene was digested by *Xba*I and *Hin*dIII, then cloned into plasmid pVT 102U/α and transformed into *Escherichia. coli* TG1 competent cells. After confirmation by sequencing, the recombinant plasmid pVT 102U/α-mutant was extracted and transformed into *S. cerevisiae* S-78 using the LiCl method (23). The expression of mutants followed the procedure described earlier (21). After fermentation, the culture supernatant was adjusted to pH 4.2 with acetic acid. Then the sample was directly applied to a CM32 cation-exchange column (2.8 × 14 cm), which was equilibrated with 0.1 M sodium acetate (pH 4.2) at a flow rate of 1 mL/min. After elution with the same buffer until a stable baseline was reached, the column was washed by stepwise elution with 0.2, 0.3 and 0.5 N NaCl in the equilibration buffer. The 0.5 N NaCl fraction was then applied directly to a reverse-phase Sephasil peptide C_{18} column. Buffer A was 0.1% trifluoroacetic acid; buffer B was 0.1% trifluoroacetic acid in acetonitrile. The C_{18} column was eluted with a linear 0–100% gradient of buffer B for 20 column volumes for M1 (C12S,C63S), or it was eluted with a linear gradient of 0–80% buffer B for 15 column volumes for M1 (C16S,C36S). Reverse-phase chromatography analysis was performed on *ÄKTA* Purifier chromatography system (Pharmacia Biotech, Sweden).

Molecular mass determination

The molecular mass of purified mutants was determined by using a Finnigan LCQ ion-trap mass spectrometer (ThermoQuest, San Jose, CA, USA) equipped with an electrospray ionization source; spray voltage was 4.50 kV. The mass calculation was performed using the program provided by the manufacturer.

Toxicity assay

Toxicity of the mutants was tested on ICR mice (male, SPF level, 18–20 g body weight), using 0.9% NaCl and rBmK M1 as negative and positive controls, respectively, and 10 mice per group. Modified samples at various doses were dissolved in 0.9% NaCl and injected into the mice through the tail vein. Survival times (time between injection and death), reaction and doses were recorded. Estimation of toxicity was based on the determination of LD_{50} (the dose capable of killing 50% of mice) according to Meier & Theakston's method (24).

Electrophysiological characterization of rBmK M1 and mutants on neuronal voltage-gated Na^+ channels ($rNa_v1.2$)

For expression in *Xenopus* oocytes, the $rNa_v1.2$ and rNaβ1 genes were subcloned into pNa200 and pSP64T plasmids. First, prior to *in vitro* transcription, $rNa_v1.2$/pNa200 and $rNa\beta1$/pSP64T were linearized by *Not*I and *Eco*RI, respectively. Then, using large-scale T7 and SP6 mMESSAGE-mMACHINE transcription kits (Ambion, USA), capped cRNAs were synthesized from the linearized plasmids. The *in vitro* synthesis of cRNA encoding $rNa_v1.2$ and $rNa\beta1$ and isolation of *Xenopus* oocytes were carried out as described previously (25). Oocytes were coinjected with 50 nL of $rNa_v1.2$ and $rNa\beta1$ cRNA each at a concentration of 1 ng/nL and a ratio of 1 : 1 using a Drummond microinjector (USA). The solution used for incubating the oocytes contained (in mM): NaCl 96, KCl 2, $CaCl_2$ 1.8, $MgCl_2$ 2 and HEPES 5 (pH 7.4), supplemented with 50 mg/L gentamicin sulfate. Whole-cell currents from oocytes were recorded 2–3 days after injection using the two-electrode voltage clamp technique.

Voltage and current electrodes were filled with 3 M KCl. Resistances of both electrodes were kept as low as possible (≈0.1–0.2 MΩ). Bath solution composition was (in mM): NaCl 96, KCl 2, $CaCl_2$ 1.8, $MgCl_2$ 2 and HEPES 5 (pH 7.4). Experiments were performed using a GeneClamp 500 amplifier (Axon Instruments, USA) controlled by a pClamp data acquisition system (Axon Instruments). Using a four-pole low-pass Bessel filter, currents were filtered at 5 kHz and sampled at 10 kHz. Digital leak subtraction of the current records was carried out using a P/2 protocol. Inactivation kinetics of Na^+ current were described by fitting the current traces between the inward peak current and the end of the pulse using the fitting procedures of PCLAMP6 software (Axon Instruments).

Data are presented as mean ± SEM. All experiments were performed at room temperature (20 ± 2°C).

Circular dichroism spectroscopy

Circular dichroism (CD) spectra were recorded on a JASCO J-720 spectropolarimeter. The mutant samples used for analyses were dissolved in 20 mM phosphate buffer (pH 7) at a concentration of 1.0 mg/mL. Spectra were run at 25°C from 250 to 190 nm by using a quartz cell of 0.5 mm length. Data were collected at 0.5 nm intervals with a scan rate of 50 nm/min. All CD spectra resulted from averaging four scans and the final spectrum was corrected by subtracting the corresponding baseline spectrum obtained under identical conditions. Spectra were smoothed by the instrument software. The secondary structure content was estimated by JASCO CD standard analysis.

Results

Mutation, expression and purification

Double mutants (C16S,C36S) (C22S,C46S) and (C26S,C48S) were created by four-step PCR (Figs 2 and 3). The mutant (C12S,C63S) was produced by one-step PCR. The target genes were expressed using the pVT 102U/α vector (Fig. 2). Tricine–SDS–PAGE analyses of cultures demonstrated that mutants (C12S,C63S) and (C16S,C36S) could be expressed

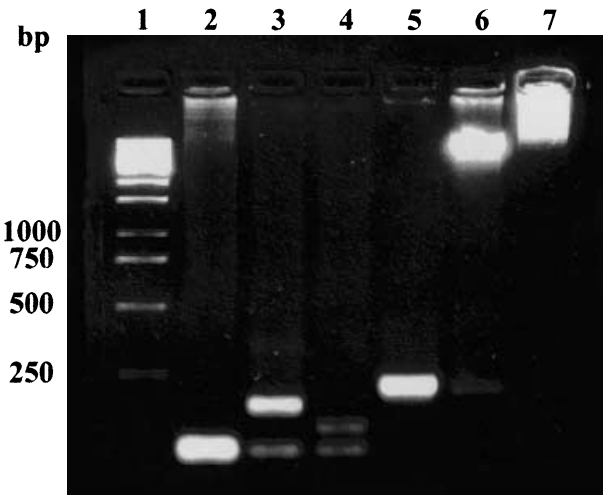

Figure 3. PCR products (2% agarose) of variant (C26S,C48S). Lane 1, 1kb DNA marker; lanes 2–5, the first to fourth PCR product; lane 6, pVT 102U/α-mutant (C26S,C48S) digested by *Xba*I and *Hin*dIII; lane 7, recombinant plasmid pVT 102U/α-mutant (C26S,C48S).

and secreted into the medium in the expression system (Fig. 5), but that (C22S,C46S) and (C26S,C48S) could not be expressed at all.

Expressed variants (C12S,C63S) and (C16S,C36S) were further purified by a simple and efficient protocol. One liter of the YPD culture was harvested and initially purified by chromatography on a CM32 column. The last step of purification was carried out on a C_{18} column (Fig. 4). The elution peaks corresponding to target mutants shown in Fig. 4 were finally pooled and lyophilized. The tricine–SDS–PAGE gels (Fig. 5) and the mass spectra (Fig. 6) showed a high purity of the final products. Chromatography profiles (Fig. 4) indicated that the expression level of mutant (C12S,C63S) was much higher than that of mutant (C16S,C36S). On average, the expression level for variant (C12S,C63S) was ≈1–2 mg/L of culture medium, which was comparable to that of unmodified rBmK M1 (≈3 mg/L). However, the purified variant (C12S,C63S) gradually decomposed during storage. For variant (C16S,C36S), the product could be purified only at trace levels due to the yield reduced markedly during the purification procedure. In the first 18 h the chromatography profile showed a definite peak on C_{18} column (Fig. 4B) and the SDS–PAGE gel showed an apparent single band (lane 2 in Fig. 5); but soon after the peak corresponding to the variant was decomposed into two peaks and the pooled sample from the main peak showed only a trace band in SDS–PAGE (lane 3 in Fig. 5). Besides, the procedure is not steady and the profile shown in Fig. 4B is the best one. We have tried the experiment several times, but could only occasionally get the result similar to that in Fig. 4B for this mutant. Therefore, with the C_{18} column (12 μm ST 4.6/250) commonly used in laboratory only a trace amount of the purified sample could be obtained finally. It indicated that the recombinant variant (C16S,C36S) could definitely be expressed and folded, but was extremely unstable.

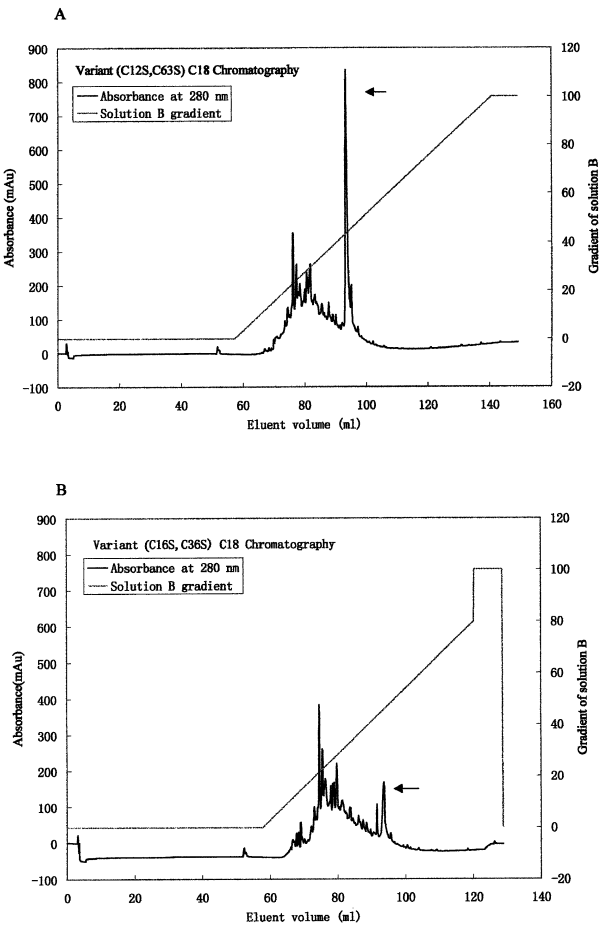

Figure 4. Purification of expressed variants (C12S,C63S) (A) and (C16S,C36S) (B) by reversed-phase chromatography on a C_{18} column. Arrows indicate peaks corresponding to the target mutants. The peak in (B) decomposed into two components after 18 h.

Molecular mass

The molecular masses of purified variants (C12S,C63S) and (C16S,C36S) were measured with the Finnigan LCQ ion

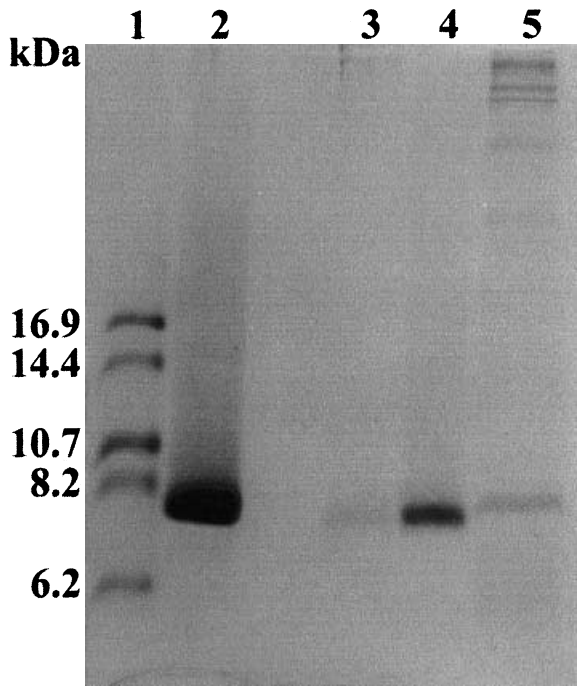

Figure 5. Tricine–SDS–PAGE of expressed variants (C12S,C63S) and (C16S,C36S) before and after purification. The protein bands were stained with Coomassie Brilliant Blue R250. Lane 1, molecular mass marker; lanes 2 and 3, purified products of variant (C16S,C36S) collected at 18 and 24 h, respectively; lane 4, purified product of variant (C12S,C63S); lane 5, fermentation supernatant of variant (C12S,C63S).

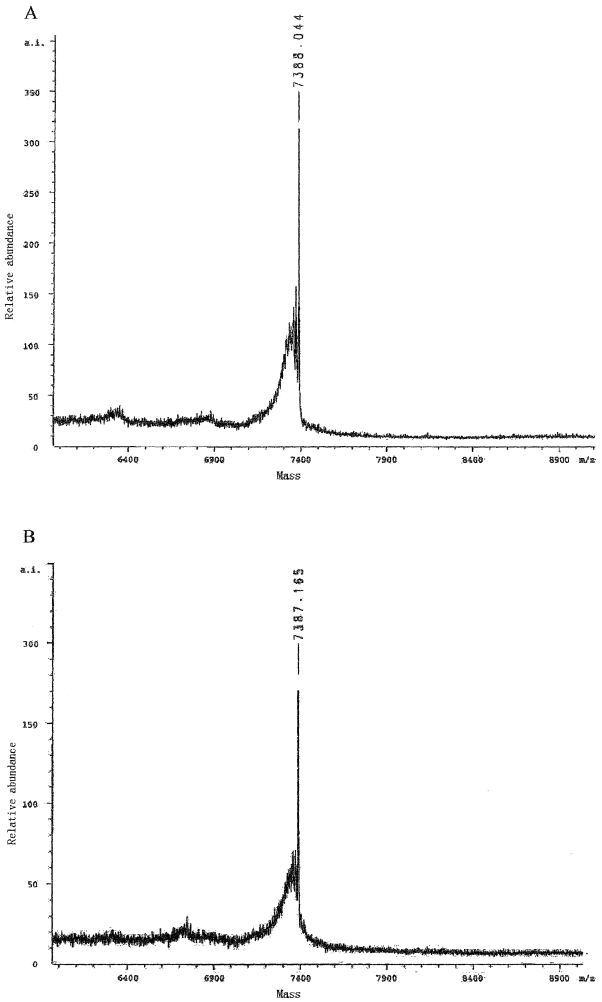

Figure 6. Finnigan LCQ ion trap mass spectrum of variants (C12S,C63S) (A) and (C16S, C36S) (B). The main peaks indicated the molecular masses of 7388.044 and 7387.165 Da for double mutants (C12S,C63S) and (C16S,C36S), respectively. They were consistent with the estimated mass value, 7389.366 Da, which showed correctness and high purity for the recombinant mutants.

trap mass spectrometer. The individual peaks definitely showed that molecular masses of variants (C12S,C63S) and (C16S,C36S) were 7388.044 and 7387.165 Da, respectively (Fig. 6). They coincided well with the estimated mass value of the mutant molecules, 7389.366 Da. The results confirmed the correct mutagenesis and the high purity of recombinant products.

Bioassay of toxic activity

After injection with unmodified rBmK M1, mice showed paralysis of rear legs first and then the whole body, loss of balance, respiratory abnormalities, incontinence of excretion and finally death, which are typical symptoms of envenomation. The LD_{50} determined according to Meier & Theakston's method (24) was ≈0.53 mg/kg (Fig. 7), which was consistent with that of the wild BmK M1 (20).

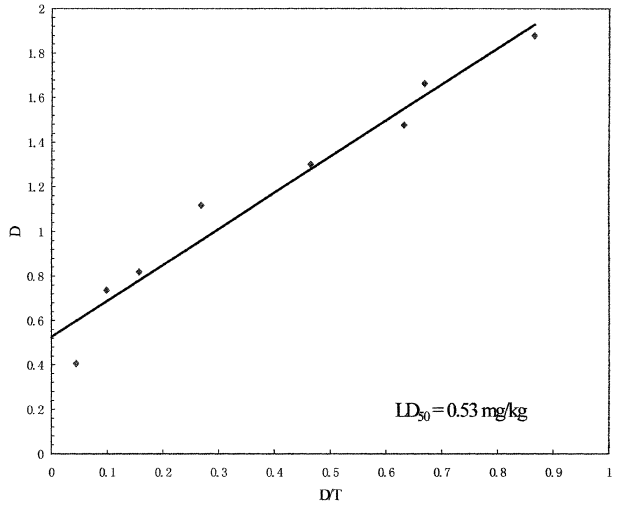

Figure 7. LD_{50} determination of rBmK M1. *D*, dose (mg/kg) of toxin used in experiments. *T*, survival time (min) of mice after injection of toxin. The LD_{50} was determined using $D - D/T$ observation. The point where the regression intersects the ordinate is the LD_{50}. The determined LD_{50} for the expressed rBmK M1 is 0.53 mg/kg.

Except for variant (C12S,C63S), the other three variants could not be used for bioassays due to either trace expression (C16S,C36S) or nonexpression, (C22S,C46S) and (C26S,C48S).

Purified variant (C12S,C63S) was injected into ICR mice through the tail vein at different doses to detect its toxic activity. No toxicity was observed even at a dose of 25 mg/kg, which is 47 times the LD_{50} of unmodified recombinant BmK M1 (Table 1). The results showed that, owing to the loss of the disulfide bond 12–63, the toxic activity was dramatically reduced.

Electrophysiological properties

The effect of rBmK M1 and rBmK M1 (C12S,C63S) on neuronal Na^+ channels ($rNa_v1.2$) expressed in *Xenopus*

***Table 1*. Summary of results for four variants with cysteine serine mutations in disulfide bonds of BmK M1**

Toxins	Expression (mg/L)	Toxicity (LD_{50}) (mg/kg)
Unmodified BmK M1	3	0.53
M1 (C12S,C63S)	1–2	>25
M1 (C16S,C36S)	Trace	–
M1 (C22S,C46S)	None	–
M1 (C26S,C48S)	None	–

oocytes are displayed in Fig. 8. Three other mutants could not be used for this experiment because of either trace expression, (C16S,C36S), or nonexpression, (C22S,C46S) and (C26S,C48S). Currents were evoked by a step depolarization to −10 mV during 25 ms from a holding potential of −90 mV. In control conditions, inactivation kinetics of $rNa_v1.2$ channels Na^+ is rapid. Current traces recorded after the addition of 1 μM rBmK M1 show that the recombinant toxin induces a slowing of the inactivation process of Na^+ currents, whereas the peak amplitude of the Na^+ current and the time to reach the peak remain unchanged. The slowing down of the inactivation kinetics of the Na^+ current is even more pronounced with a higher concentration of rBmK M1 (5 μM). Interestingly, the double mutated toxin M1 (C12S,C63S), even at a higher concentration (100 μM), is unable to induce any change of the inactivation kinetics of $rNa_v1.2$. The time constant of inactivation (tau) calculated by a single exponential fit increases from 2.2 ± 0.3 ms ($n = 11$) in control conditions to 3.0 ± 0.4 ms ($n = 7$) and 4.4 ± 0.2 ms ($n = 3$) after the addition of 1 and 5 μM rBmK M1, respectively. This represents an increase for the time constant of inactivation of ≈36 and 99% in the presence of 1 and 5 μM rBmK M1, respectively. Student's *t*-test indicates that tau-values measured in the presence of both concentrations of rBmK M1 are significantly different ($P < 0.01$). In contrast, in the presence of 100 μM M1 (C12S,C63S), the time constant of inactivation, 2.3 ± 0.3 ms ($n = 6$), remains almost the same as in control conditions.

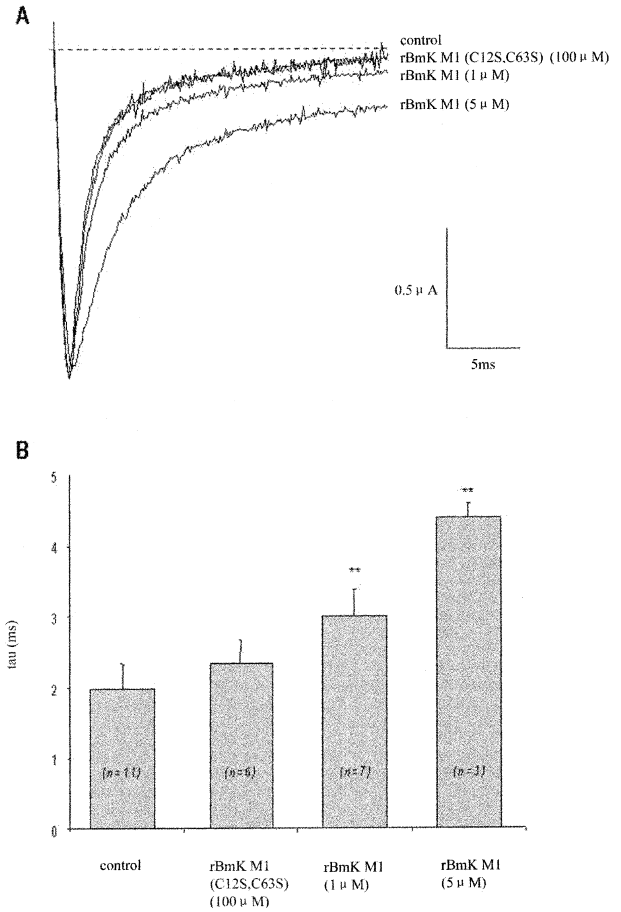

Figure 8. Effect of rBmK M1 and rBmK M1 (C12S,C63S) on inactivation kinetics of Na channels expressed in *Xenopus* oocytes. (A) Current traces after coexpression of $rNa_v1.2$ and rNaβ1 in *Xenopus* oocytes were evoked by a step depolarization to −10 mv during 25 ms from a holding potential of −90 mv, in the absence (control) and in the presence of 100 μM rBmK M1 (C12S,C63S), 1 or 5 μM rBmK M1 (as indicated). Note the absence of effect of the mutated toxin at high concentration as compared with the slowing of inactivation time course induced by the wild-type toxin. (B) Histograms to display time constants of inactivation of Na^+ currents in the absence (control) and in the presence of 100 μM rBmK M1 (C12S,C63S), 1 or 5 μM rBmK M1. Time constants of inactivation were calculated from a single exponential fit of current traces. Data represent the mean ± SEM of *n* experiments (as mentioned). Asterisks indicate that values are significantly different ($P < 0.01$).

Conformational analysis

Only the purified variant (C12S,C63S) could be supplied to CD experiment, because the yield of recombinant variant (C16S,C36S) was obtained in trace amounts after purification (Table 1). CD spectra of variant (C12S,C63S) and unmodified BmK M1 in the UV range of 250–190 nm were shown in Fig. 9. The secondary structure estimation (J-700 for Windows Secondary Structure Estimation, Version 1.10.00) showed that, compared with native M1, in variant (C12S,C63S) the helix is not changed (from 5.4 to 5.8%), but the β structure is reduced ≈16% (from 86.1 to 69.9%) and the random coil is increased ≈15.7% (from 8.6 to 24.3%). The results indicated that the framework of the native

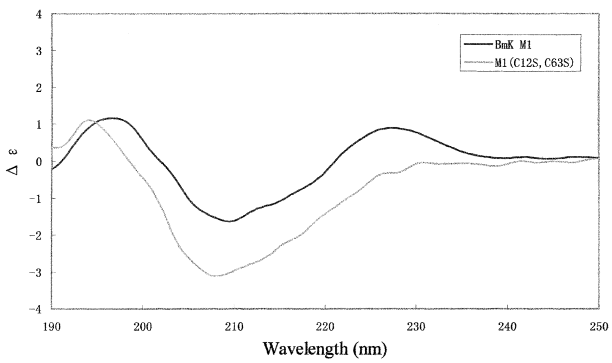

Figure 9. CD spectra of variant (C12S,C63S) and unmodified BmK M1. The measurement is carried out in the UV range 250–190 nm on a Jasco 720 system at pH 7.0 with a concentration of 1.0 mg/mL at room temperature.

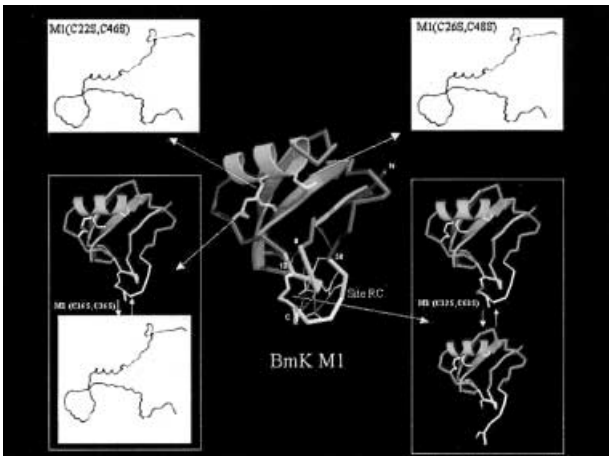

Figure 10. Schematic drawing of the consequence of the removal of four disulfide bonds in the scorpion toxin BmK M1. The native scaffold of BmK M1 determined by X-ray analysis (8) is shown in the center and the four disulfide bonds modified in experiments are highlighted by arrows. The details are described in the text.

structure should be basically maintained but much loose in the mutant. It is plausible to predict that the loosed part of the variant is probably at the Site RC as shown in Fig. 10, where the disulfide bond C12–C63 with a complicated hydrogen bond network cross-links a five-residue reverse turn with the C-terminal segment to form a unique tertiary unit. The lose of this disulfide bridge would certainly influence the conformational stability of this part and made the tertiary structure of the variant more loose than that in the native. As described above, purified variant (C12S,C63S) could be decomposed during storage. The instability observed in the experiment is well coincident to the result from CD analyses.

Discussion

Although one can generally predict that all disulfide bonds in the scorpion toxins are significant, there is no information about the respective roles for these disulfide bonds. Understanding these roles will benefit the use of scorpion toxins as natural scaffold in protein engineering. The roles of four disulfide bonds in the BmK scorpion toxin have been distinguished in this report by mutagenesis analyses.

C22–C46 and C26–C48 are essential for general folding

X-Ray structural analysis (8) of BmK M1 revealed a dense core of secondary structure elements, including an α-helix formed by residues 19–28 and an antiparallel three-stranded β-sheet formed by residues 2–5, 32–37 and 45–51, as depicted in Fig. 10. The secondary structures are mainly cross-linked by three disulfide bonds, C16–C36, C22–C46 and C26–C48. Two of them, C22–C46 and C26–C48 link the α-helix to the third strand of the β-sheet and the third, C16–C36, links the large loop between the first β-strand and the α-helix to the second β-strand (Fig. 10).

In a suitable expression system which has successfully expressed native BmK M1 (21) and variant (C12S,C63S) (in this study), mutants (C22S,C46S) and (C26S,C48S) cannot be expressed at all. This result indicates that without disulfide bonds 22–46 or 26–48 the polypeptide chain of the BmK toxin could not be folded at all. These two disulfide bridges are essential for the general folding of toxins. It seems that the α-helix (residues 19–28) linking with the β-strand (residues 45–51) by C22–C46 and C26–C48 to form a αβ motif is a crucial step in the folding. This stable motif should be the core of the molecular scaffold. Therefore, disulfide bonds 22–46 and 26–48 are absolutely needed for any mimics or modeling using the scorpion toxin as scaffold.

C16–C36 is crucial for the overall stability of the folded molecule

The chromatographic analysis (Fig. 4) and mass spectroscopy (Fig. 6) showed that variant M1 (C16S,C36S) could be expressed at a trace level. The observation in this experiment indicated that without disulfide bond 16–36, the mutated molecule could correctly be folded temporarily, but it is extremely unstable. It implies that the removal of disulfide bond 16–36 does not fatally impact on the general folding of the toxin, but evidently reduces the stability of the folded molecule. Thus, this bridge is a crucial structural element for stabilizing the general fold. Actually the disulfide bond 16–36 links a long loop between strand β_1- and α-helix to the strand β_2 which is in between β_3 and α-helix (Fig. 10). Through six main-chain hydrogen bonds (8), the strand β_2 connected with the strand β_3 to form a βαβ motif. This motif will be rather flexible without the bridge C16–C36, therefore the stability of the folded state will seriously be reduced.

C12–C63 is critical for the functional performance

Interestingly, the recombinant M1 (C12S,C63S) can be expressed in an amount comparable with that of the native rBmK M1 (Table 1). This result indicates that the disulfide

bond 12–63 is not fatal for the general fold of the toxin molecule. In fact, this disulfide bridge is more solvent exposed than three others on the molecular surface (Fig. 10) and shows variable conformations in different toxin structures [e.g. AaH II (6), Lqq III (26), BmK M8 (7)] exhibiting a certain flexibility of this bridge. However, the gradual degradation observed in the purified variant M1 (C12S,C63S) indicates that the disulfide bridge 12–63 is also a factor for stabilizing the local structure, Site RC, of the native molecule. Nevertheless, both the bioassay *in vivo* and the electrophysiological characterization on neuronal Na^+ channels show that recombinant M1 (C12S,C63S) has no detectable bioactivities (Table 1 and Fig. 8). The result demonstrates that the disulfide bond 12–63 is essential for the toxic activity and the binding property with the Na^+ channel of the native molecule. The detailed structural analysis and comparison (7,8) revealed that a five-residue turn 8–12 is cross-linked with the C-terminal segment 58–63 by the disulfide bridge 12–63 and a hydrogen bond network to form a unique tertiary arrangement, the site RC (see Fig. 10), which is crucial for the toxin-receptor binding. Evidently, the loss of this bridge will destroy the subtle tertiary arrangement of this part. This may be a structural reason for the loss of the toxic activity. In this way, the disulfide bond 12–63 plays an important role in the functional performance of the native toxin.

Considering the four disulfide bonds appearing in BmK M1 are conservative in all long chain α-toxins (see Fig. 1), the conclusion drawn from the mutagenesis analyses of BmK M1 may also be generalized to other toxins.

Acknowledgements: This work was supported by the State Basic Research Program (G19990756), the National Natural Science Foundation (39970158) of China and a bilateral grand between China and Flanders (BIL00/04). The rNa$_v$1.2 and rNaβ1 clones were kindly donated by A. Goldin and S.H. Heinemann, respectively.

References

1. Gordon, D. (1997) Sodium channels as targets for neurotoxins: mode of action and interaction of neurotoxins with receptor sites on sodium channels. In *Toxins and Signal Transduction, Cellular and Molecular Mechanisms of Toxin Action Series* (Lazarovici, P. & Gutman, Y., eds). Harwood Press, Amsterdam, pp. 119–149.
2. Miller, C. (1995) The charybdotoxin family of K^+ channel-blocking peptides. *Neuron* **15**, 5–10.
3. Lippens, G., Najib, J., Wodak, S.J. & Tartar, A. (1995) NMR sequential assignments and solution structure of chlorotoxin, a small scorpion toxin that blocks chloride channels. *Biochemistry* **34**, 13–21.
4. Martin-Eauclaire, M.F. & Couraud, F. (1995) Scorpion neurotoxins: effects and mechanisms. In *Handbook Neurotoxicology* (Chang, L.W. & Fyer, R.S., eds). Marcel Decker, New York, pp. 683–716.
5. Delepierre, M., Prochnicka-Chalufour, A. & Possani, L.D. (1997) A novel potassium channel blocking toxin from the scorpion *Pandinus imperator*: a ^{1}H NMR analysis using a nano-NMR probe. *Biochemistry* **36**, 2649–2658.
6. Housset, D., Habersetzer-Rochat, C., Astier, J.P. & Fontecilla-Camps, J.C. (1994) Crystal structure of toxin II from the scorpion *Androctonus australis* Hector refined at 1.3 Å resolution. *J. Mol. Biol.* **238**, 88–103.
7. Li, H.M., Wang, D.C., Zeng, Z.H., Jin, L. & Hu, R.Q. (1996) Crystal structure of an acidic neurotoxin from scorpion *Buthus martensii* Karsch at 1.85 Å resolution. *J. Mol. Biol.* **261**, 415–431.
8. He, X.L., Li, H.M., Zeng, Z.H., Liu, X.Q., Wang, M. & Wang, D.C. (1999) Crystal structures of two α-like scorpion toxins: non-proline *cis* peptide bonds and implications for new binding site selectivity on the sodium channel. *J. Mol. Biol.* **292**, 125–135.
9. Wang, D.C. (1999) A series of bioactivity-variant neurotoxins from scorpion *Buthus martensii* Karsch: X-ray crystal structure and functional implications. *J. Nat Toxins* **8**, 309–325.
10. Gordon, D., Savarin, P., Gurevitz, M. & Zinn-Justin, S. (1998) Functional anatomy of scorpion toxins affecting sodium channels. *J. Toxicol. Toxin Rev.* **17**, 131–159.
11. Cornet, B., Bonmatin, J.M., Hetru, C., Hoffmann, J.A., Ptak, M. & Vovelle, F. (1995) Refined three-dimensional solution structure of insect defensin A. *Structure* **3**, 435–448.
12. Bruix, M., Jiménez, M.A., Santoro, J., González, C., Colilla, F.J., Méndez, E. & Rico, M. (1993) Solution structure of γ1-H and γ1-P thionins from barley and wheat endosperm determined by ^{1}H-NMR: a structural motif common to toxic arthropod proteins. *Biochemistry* **32**, 715–724.
13. Gao, G.H., Dai, J.X., Ding, M., Hellekant, G., Wang, J.F. & Wang, D.C. (1999) Solution conformation of brazzein by ^{1}H nuclear magnetic resonance: resonance assignment and secondary structure. *Int. J. Biol. Macromol.* **24**, 351–359.
14. Caldwell, J.E., Abildgaard, F., Dzakula, Z., Ming, D., Hellekant, G. & Markley, J.L. (1998) Solution structure of the thermostable sweet-tasting protein brazzein. *Nat. Struct. Biol.* **5**, 427–431.
15. Vita, C., Roumestand, C., Toma, F. & Ménez, A. (1995) Scorpion toxins as natural scaffolds for protein engineering. *Proc. Natl Acad. Sci. USA* **92**, 6404–6408.
16. Vita, C. (1997) Engineering novel proteins by transfer of active sites to natural scaffolds. *Curr. Opin. Biotechnol.* **8**, 429–434.
17. Ji, Y.H., Mansuelle, P., Terakawa, S., Kopeyan, C., Yanaihara, N., Xu, K. & Rochat, H. (1996) Two neurotoxins (BmK I and BmK II) from the venom of the scorpion *Buthus martensii* Karsch: purification, amino acid sequence and assessment of specific activity. *Toxicon* **34**, 987–1001.
18. Li, Y.J. & Ji, Y.H. (2000) Binding characteristics of BmK I, an alpha-like scorpion neurotoxic polypeptide, on cockroach nerve cord synaptosomes. *J. Peptide Res.* **56**, 195–200.

19. Possani, L.D., Becerril, B., Delepierre, M. & Tytgat, J. (1999) Mini Review: Scorpion toxins specific for Na^+-channels. *Eur. J. Biochem.* **264**, 287–300.
20. Li, H.M., Zhao, T., Jin, L., Wang, M., Zhang, Y. & Wang, D.C. (1999) A series of bioactivity-variant neurotoxins from scorpion *Buthus martensii* Karsch: purification, crystallization and crystallographic analysis. *Acta Crystallogr.* **D55**, 341–344.
21. Shao, F., Xiong, Y.M., Zhu, R.H., Ling, M.H., Chi, C.W. & Wang, D.C. (1999) Expression and purification of the BmK M1 neurotoxin from the scorpion *Buthus martensii* Karsch. *Protein Expr. Purif.* **17**, 358–365.
22. Xiong, Y.M., Ling, M.H., Wang, D.C. & Chi, C.W. (1997) The cDNA and genomic DNA sequences of a mammalian neurotoxin from the scorpion *Buthus martensii* Karsch. *Toxicon* **35**, 1025–1031.
23. Ito, H., Fukuda, Y., Murata, K. & Kimura, A. (1983) Transformation of intact cells treated with alkali cations. *J. Bacteriol.* **153**, 163–168.
24. Meier, J. & Theakston, R.D.G. (1986) Approximate LD_{50} determinations of snake venoms using eight to ten experimental animals. *Toxicon* **24**, 395–401.
25. Liman, E.R., Tytgat, J. & Hess, P. (1992) Subunit stoichiometry of a mammalian K^+ channel determined by construction of multimeric cDNAs. *Neuron* **9**, 861–871.
26. Landon, C., Cornet, B., Bonmatin, J.M., Kopeyan, C., Rochat, H., Vovelle, F. & Ptak, M. (1996) ^1H NMR-derived secondary structure and the overall fold of the potent anti-mammal and anti-insect toxin III from the scorpion *Leiurus quinquestriatus quinquestriatus*. *Eur. J. Biochem.* **236**, 395–404.